Jul 1st, 12:00 AM

Geomechanical modelling of triggering mechanisms for rainfall-induced triangular shallow landslides of the flow-type

L. Cascini

S. Cuomo

M. Pastor

J. A. Fernández-Merodo

iEMSs 2008: International Congress on Environmental Modelling and Software
Integrating Sciences and Information Technology for Environmental Assessment and Decision Making
4th Biennial Meeting of iEMSs, http://www.iemss.org/iemss2008/index.php?n=Main.Proceedings
M. Sànchez-Marrè, J. Béjar, J. Comas, A. Rizzoli and G. Guariso (Eds.)
International Environmental Modelling and Software Society (iEMSs), 2008

Geomechanical modelling of triggering mechanisms for rainfall-induced triangular shallow landslides of the flow-type

L. Cascini[a], S. Cuomo[a], M. Pastor[b], J.A. Fernández-Merodo[b]

[a] University of Salerno, Department of Civil Engineering, Italy
(l.cascini@unisa.it, scuomo@unisa.it)
[b] Centro de Estudios y Experimentación de Obras Públicas (CEDEX), Madrid, Spain
(mpastor@cedex.es, jose.a.fernandez@cedex.es)

Abstract: Landslides of the flow-type are frequently triggered by rainfall as shallow landslides in different types of soils and geo-environmental contexts. When involving open slopes, these landslides often occur in triangular source areas where initial slides turn into avalanches through further failures and/or eventual soil entrainment. Similar phenomena are frequently observed in layered snow deposits and they are also recognised in ashy deposits on Mars. Significant examples are systematically recorded in Southern Italy where pyroclastic deposits overlie carbonate massifs. Particularly, in May 1998, rainfall triggered many destructive triangular shallow landslides of the flow-type along the slopes of Pizzo d'Alvano massif (Sarno-Quindici event). The available data-set allowed their failure and post-failure stages to be modelled. Numerical analyses were performed using limit equilibrium as well as hydro-mechanical coupled and uncoupled stress-strain approaches. The obtained results are discussed in the paper, providing a preliminary framework for this type of slope instability phenomena that is poorly addressed in the current literature.

Keywords: Rainfall, Shallow landslides, Flow-type, Triangular source areas, Avalanche.

1. INTRODUCTION

Landslides of the flow-type [Hungr et al., 2001, Pastor et al., 2008], when involving open slopes, frequently originate as small landslides (failure stage) that increase their initial volumes in triangular-shaped areas (post-failure stage) according to complex mechanisms not yet completely understood [Chen et al., 2006; Crosta et al., 2006]. Similar phenomena are often observed in layered snow deposits [Jamieson & Stethem, 2002] where different snow avalanches occur in relation to in-situ and climate conditions [Pielmeier et al., 2003]. Triangular avalanche phenomena were also recognised in some ashy deposits on Mars, where high resolution images [Gerstell et al., 2004] highlight the presence of impact craters at the head of the scars.

In shallow soil deposits, the failure stage of triangular-shaped landslides triggered by rainfall is associated with different triggering factors. Karst springs from bedrock are recognised as a possible cause [Cascini et al., 2005, 2008; Di Crescenzo & Santo, 2005] with significant examples for pyroclastic deposits of Southern Italy discussed by Budetta & de Riso [2004] and Guadagno et al. [2005]. Another triggering factor is the impact of failed soil masses on stable deposits [Hutchinson & Bhandari, 1971] with major examples available for torrent deposits in USA [Costa & Williams, 1984], for decomposed granitic soils in Japan [Wang et al., 2003] and for pyroclastic deposits in Southern Italy [Guadagno et al., 2005; Di Crescenzo & Santo, 2005]. The transition from initial slides to avalanches [Hungr et al., 2001] can be related to soil/material entrainment along the path of the failed masses [Jakob and Hungr, 2005; Crosta et al., 2006]. The increase of the initial failed volumes can be also associated with further failures occurring inside the landslides source

areas. Examples are available for events occurred in Southern Italy [Cascini, 2005, 2008, Cuomo, 2006] and for snow deposits [Pielmeier et al., 2003]. Moreover, the transition from slide to avalanche can be connected to liquefaction phenomena. In the literature, contributions based on theoretical evaluations and laboratory tests are available on the topic [Wang et al., 2003].

Due to the catastrophic consequences that these phenomena generally cause [Cascini et al., 2005], the understanding and modelling of both the failure and post-failure stages are a fundamental issue in mitigating the posed risk to life and facilities. The paper addresses this topic using different geomechanical approaches, with reference to a study area (Sarno-Quindici, Southern Italy) where disastrous events were recently recorded.

2. CASE STUDY

2.1 Landslides event

Shallow landslides of the flow-type have been systematically recorded for many centuries [Guadagno et al., 2005] in a populated area of Southern Italy where unsaturated pyroclastic soils [Cascini & Sorbino, 2002] overlie carbonate massifs. Particularly, on 4-5 May 1998, many destructive landslides of the flow-type were triggered by heavy rainfall [Cascini et al., 2000; Fiorillo & Wilson, 2004], causing 159 fatalities and relevant damage to property. Different and complex triggering mechanisms were recognised [Cascini et al., 2005, 2008]. One of the most frequent triggering mechanism (M2) was associated with triangular landslide source areas by Cascini et al. [2005, 2008]. The source areas are a few meters wide near the bedrock scarps and downwards enlarging (Fig. 1a). For these landslides, Cascini et al. [2008] recognised the karst springs from the bedrock (scheme M2a) and the impact of failed soil masses on stable deposits (scheme M2b) as the main triggering factors (Fig. 1b). However, also for the latter ones (scheme M2b), the presence of a karst spring was recognised as a necessary condition for the downwards enlargement of the impacted zone at the base of the scarps. Particularly, Cascini et al. [2008] observed that, in both cases, karst spring were only active for short periods of time (less than 24 hours) when they also had a high discharge (up to 10^{-4} m/s). On the other hand, the impact phenomena were related to small volumes of failed soil masses (10 - 100 m^3) falling from bedrock scarps (2 – 20 m tall). Figure 1c shows the areal distribution of the triangular-shaped phenomena that occurred in the study area in May 1998 [Cascini et al., 2008].

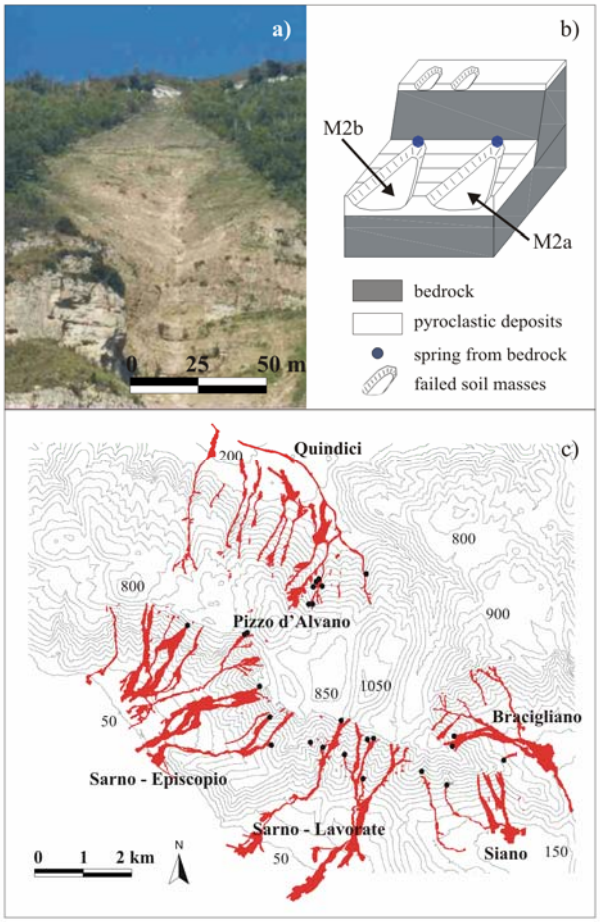

Figure 1. Triangular shallow landslides of flow-type occurred in the study area on May 1998.

2.2 Literature review

Despite their catastrophic consequences, these landslides are not exhaustively discussed in the literature as far as their failure and post-failure stages are concerned. Among the available contributions, morphometrical analyses suggest that landslides crown zones are characterised by apical angles ranging between 15° and 30° and steepness from 35° to 45° [Di Crescenzo & Santo, 2005]. However, similar analyses show that the geometrical features of the landslides source areas (apex angle of the source areas, height of natural and anthropogenic scarps, slope length, slope angle, initial volume) can be poorly correlated with each other [Guadagno et al., 2005].

These landslides have not been exhaustively modelled. Among the available contributions, Calcaterra et al. (2004) show that karst springs from bedrock affect the groundwater regime in large portions of the pyroclastic deposits (2-12 m in length) after 6-24 hours. However, the consequential slope failures are not analysed or modelled. On the other hand, Guadagno et al. [2003] highlight the role of bedrock scarps for upslope failures while slope instabilities occurring downslope the scarps are not addressed. As a contribution to the topic, the paper proposes a rational framework for geomechanical modelling aimed at investigating the failure and post-failure stages of the phenomena occurred in May 1998.

2.3 Proposed approaches, in-situ conditions and soil properties

The failure stage associated with springs from bedrock (scheme M2a) can be profitably analysed through an hydro-mechanical uncoupled approach. This approach is firstly based on pore water pressures modelling in saturated-unsaturated conditions through the numerical integration of the well-known Richards' equation. The obtained results can be then used as input to perform limit equilibrium analyses that relate the failure onset to slope safety factors approaching to one. To this aim, a rigid-perfectly plastic model can be adopted with a Mohr-Coulomb criterion extended to unsaturated conditions [Fredlund et al., 1978]. Referring to the same pore water pressures, stress-strain analyses can also be performed to validate the previous findings. Particularly, an elastic-perfectly plastic soil model can be used and both equilibrium and compatibility equations can be taken into account for the landsliding masses.

Failures induced by impact phenomena on stable deposits (scheme M2b) can be investigated using the above mentioned uncoupled approach, under the assumption of drained conditions. Conversely, if undrained conditions are considered, the excess pore water pressures must be necessarily evaluated referring, for instance, to the total isotropic and deviatoric stress variations respectively through the pore pressure coefficients α and β [Henkel, 1960]. Alternatively, hydro-mechanical coupled approaches [Pastor et al., 2002] can be used to take into account the effects of soil deformations on pore water pressures.

For the post-failure stage of these landslides, geomechanical modelling can be rigorously performed through hydro-mechanical coupled approaches that represent powerful tools especially when advanced soil constitutive models are available. However, uncoupled stress-strain analyses can be also used to investigate, under simplified assumptions, some aspects of the post-failure stage.

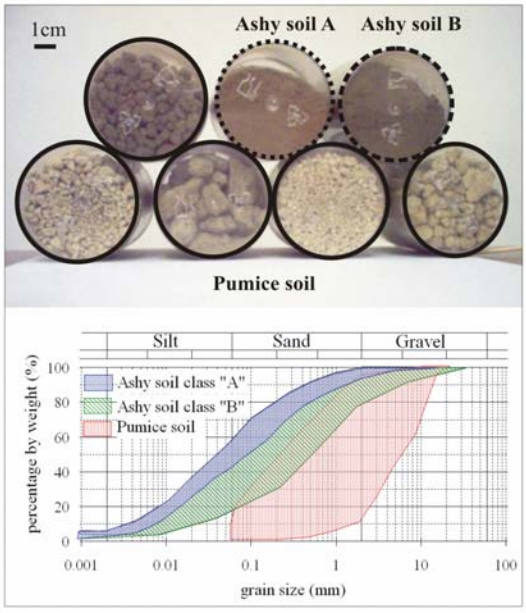

Figure 2. Pyroclastic soils from the study area.

The analyses discussed in the following sections were carried out on the available data-set that refers to both in-situ conditions and soil properties. As it concerns in-situ conditions, the typical stratigraphies consist of alternating layers (0.2-2m thick) that, as recognised by Cascini et al. [2005], belong to three main soil classes [Bilotta et al., 2005] i.e. pumice soils, coarser superficial ashy soils (class B) and finer deep ashy soil (class A) (Fig. 2).

As for the soil mechanical properties in saturated and unsaturated conditions, the literature provides soil water content and conductivity curves as well as the shear strength and stiffness [Bilotta et al., 2005] for typical suction values measured during the whole hydrological year [Cascini & Sorbino, 2002]. Typical values of the geotechnical properties are summarised in table 1.

Table 1. Soil mechanical properties.

	γ_d (kN/m^3)	γ_{sat} (kN/m^3)	n (-)	k_{sat} (m/s)	c' (kPa)	φ' (°)	φ^b (°)	ν (-)	E (MPa)	ψ (°)
Class B ashy soil	7.30	13.1	0.58	10^{-5}	0 ÷ 5	36 ÷ 41	20	0.26	5 ÷ 7	10 ÷ 20
Pumice soil	6.20	13.1	0.69	10^{-4}	0	37	20	-	-	-
Class A ashy soil	9.10	15.7	0.66	10^{-6}	5 ÷ 15	32 ÷ 35	20	0.30	1 ÷ 3	10 ÷ 20

3. PRELIMINARY GEOMECHANICAL MODELLING

3.1 Failure stage: the role of karst springs from bedrock

Using the uncoupled approach discussed in sect. 2.3 and the field data on karst springs from the bedrock (sect. 2.1), pore water pressures were computed through the Seep/W Finite Element code [Geoslope, 2004] for time periods shorter than 48 hours referring to the typical stratigraphies of the pyroclastic deposits (schemes 1-3 in Fig. 3) and soil mechanical properties listed in table 1. For each scheme, the initial conditions were assessed through a preliminary transient seepage analysis over the period January 1, 1998 – May 3, 1998. Unsaturated soil conditions were simulated throughout the slope section. The hydraulic boundary conditions were selected as follows: i) measured rainfall values at the ground surface [Cascini et al., 2008], ii) impervious boundary at the contact between bedrock and pyroclastic deposits; iii) water flux or hydrostatic distribution at upper lateral boundary of the pyroclastic deposits due to the presence of a karst spring. The achieved results outline that karst spring induces transient pore water pressures with maximum simulated values equal to 30 kPa for scheme 1 containing only class B ashy soils and 40 kPa for scheme 2 including class A and B ashy soils (Fig. 3). Similar results were obtained assuming hydrostatic distributions of pore water pressures at the upper lateral boundary of the deposits (i.e. corresponding to fractures 1.8 – 4.5 m deep), so highlighting the stratigraphy as a key factor in the groundwater regime. Particularly, ashy A soils strongly increase the simulated pore water pressures (scheme 2 in Fig. 3) while pumice soil layers determine an enlargement of the slope portion affected by the presence of springs (scheme 3 in Fig. 3).

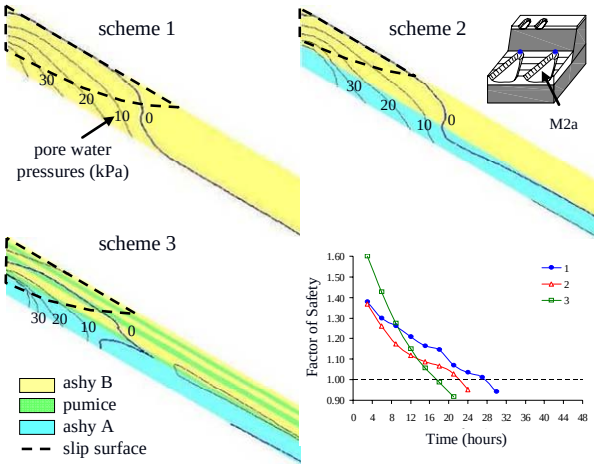

Figure 3. Failure stage induced by karst springs from

Once the pore water pressure regime was evaluated, the failure onset was investigated with limit equilibrium analyses, through the Slope/W code [Geoslope, 2004]. Planar

and curvilinear slip surfaces were considered. The curvilinear slip surfaces are associated to the minimum safety factors. Particularly, failure conditions were simulated assuming low discharges (3×10^{-5} m/s) over short time periods (> 20 h). Similar results were obtained by considering hydrostatic pore water pressure distributions at the upper lateral boundary of the pyroclastic deposit. In all the cases analysed, failed volumes depend on pore water pressures and soil shear strength properties, that are both strictly related to stratigraphy (Fig. 3). The latter is therefore outlined as a key factor for landsliding. The obtained results are confirmed by stress-strain analyses [Cuomo, 2006] performed using the Sigma/W Finite Element code [Geoslope, 2004], assuming an elastic-perfectly plastic constitutive model and soil properties in table 1. For instance, for the scheme 1, the simulated strains concentrate at the bedrock-cover contact well matching the slip surfaces assumed in the limit equilibrium analyses.

3.2 Failure stage: the role of impact of failed soil masses on stable deposits

This triggering mechanism was investigated, in static conditions, through a parametric analysis. As for the stratigraphy, the schemes of sect. 3.1 were considered. Impact loading pressures were estimated through the procedure proposed by Wang et al. [2003], referring to typical values for the heights of bedrock scarps and failing volumes (sect. 2.1). Impact loading pressures were so estimated as ranging between 5 kN/m and 30 kN/m. Moreover, distinct initial pore water pressures were considered, being related to the season and the eventual presence of karst springs from the bedrock.

Geomechanical modelling was firstly performed assuming drained conditions. As initial conditions, pore water pressures were assumed equal to those obtained with the previous transient seepage analysis over the period January 1, 1998 – May 3, 1998. Uniform distributions of pore water pressures were also considered with values ranging between 5 kPa and 60 kPa, that are the extreme values recorded during the in-situ investigations [Cascini & Sorbino, 2002]. Limit equilibrium analyses were performed through the Slope/W code, assuming uniform impact loading pressures. Curvilinear and planar slip surfaces were referred. The planar slip surfaces are associated to the minimum safety factors. The failure onset was not simulated, independently from the considered stratigraphy, pore water pressure and impact loading pressure. In fact, the impact loading pressures increase both the driving and resistance forces for the assumed slip surfaces essentially due to the slope geometry and loading conditions. As a consequence, slope safety factors change slightly with load application and achieve their initial value on load removal. As an example, figure 4 shows the results obtained for different stratigraphies and pore water pressures equal to those simulated at May 3, 1998.

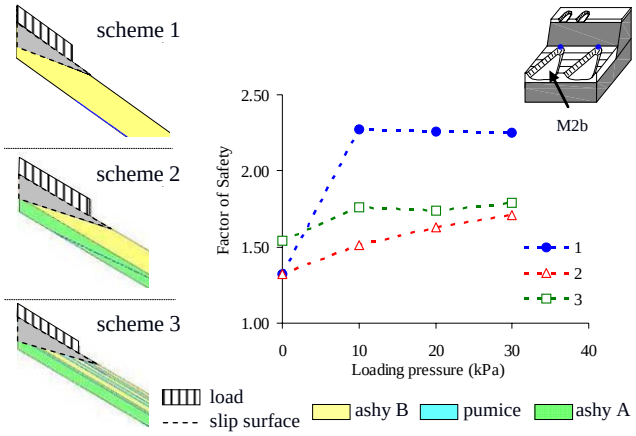

Figure 4. Effects of impact phenomena in drained conditions.

Based on the same pore water pressures, stress-strain analyses [Cuomo, 2006] outline the highest deformations in portions of the slope well matching the critical slip surfaces (Fmin) computed with the limit equilibrium analyses. Moreover, failure conditions are not predicted by the numerical analysis for any initial pore water pressure distribution.

Geomechanical modelling was then performed assuming that during the impact phenomena undrained conditions can exist. Referring to the uncoupled approach discussed in sect. 2.2, impact-induced variations of total stresses were firstly computed using the Sigma/W code.

Then, assuming nearly saturated soil conditions for suction values up to 5 kPa ÷ 10 kPa, for the ashy soils, the coefficient α was estimated (between 0.33 and 1) while the coefficient β was assumed equal to one. Finally, impact-induced pore water pressures variations were computed referring to the variations of total stresses and α, β coefficients. The performed analyses outline that deviatoric stresses strongly increase in the impact zone. Conversely, effective isotropic stresses significantly decrease due to the build up of the pore water pressures (Fig. 5). Indeed, the latter ones reach high values that are related to the soil stiffness, applied loading pressures and initial conditions. As a consequence, liquefaction phenomena may also occur. However, the accurate numerical modelling of these phenomena requires the use of advanced soil constitutive models whose calibration for these soils is not available in current literature. Consequently, a rigid-perfectly plastic constitutive model was consider first. Using this model, limit equilibrium analyses were performed assuming the stratigraphies of sect. 3.1 and the pore water pressures previously computed in undrained conditions. The example provided in figure 5a refers to scheme 1 of figure 3 (ashy B soils), having α and β respectively equal to 0.5 and 1, and initial pore water pressures equal to those computed on May 3, 1998. The obtained results outline that the slope safety factor, at load application, is still higher than unity (F=1.531), notwithstanding the increase of pore water pressures. Conversely, at loading removal, the same pore water pressures correspond to failure conditions (F=0.989). Similar slope instability scenarios can be drawn considering an initial suction value equal to 5kPa.

To validate the previous findings, the hydro-mechanical coupled approach proposed by Pastor et al. [2002] was used considering an elastic-perfectly plastic constitutive model. The obtained results match the previously simulated slope instability scenarios well as it concerns both pore water pressures and plastic strains. 3D stress-strain analyses also outline that the initial stress field is significantly modified by the assumed impact loading pressures. Particularly, the highest shear stresses (σ_{yz}) mainly concentrate along a direction forming an angle of 15-45° with the x-direction and plastic strains arise in a zone downslope enlarging (Fig. 5b).

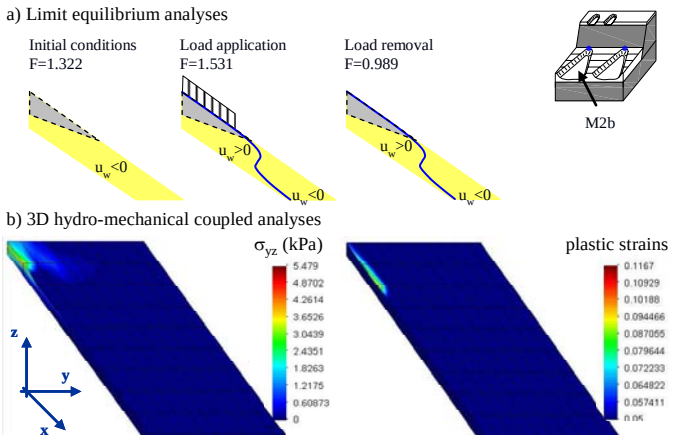

Figure 5. Effects of impact phenomena in undrained conditions.

3.3 An interpretation for the post-failure stage

The geomechanical modelling of the post-failure stage was performed using the simplified hydro-mechanical uncoupled approach discussed in sect. 2.2. To this aim, stress-strain analyses were performed referring, in static conditions, to planes parallel to the ground surface (s-y planes in Fig. 6). In these planes, at different depths, stresses along the longitudinal s-direction and lateral y-direction depend on slope angles and soil mechanical properties. At the upper boundary of these planes, loading pressures (σ_L) were assumed to be downwards applied along the longitudinal s-direction, to simulate the presence of a failed mass pushing the stable deposits downslope. The obtained results show that the applied loading pressures (σ_L) heavily modify the stress and strain fields in the s-y planes. Particularly, deviatoric stresses significantly increase and shear strains mainly concentrate along special directions that can be related to the stresses acting along the longitudinal s-direction and lateral y-direction. Yielding conditions were predicted by the numerical analysis over large portions of the slope, also for low pressures (< 20 kN/m) applied at the

upper boundary of the s-y planes, essentially due to the initial low lateral stresses (σ_y) along the y-direction. However, the lateral enlargement of the yielded zone is related to the stresses acting along both longitudinal and lateral directions. High longitudinal stresses (σ_s) predispose the arising of yielding conditions while initial high lateral stresses (σ_y) restrain the effects of the applied load.

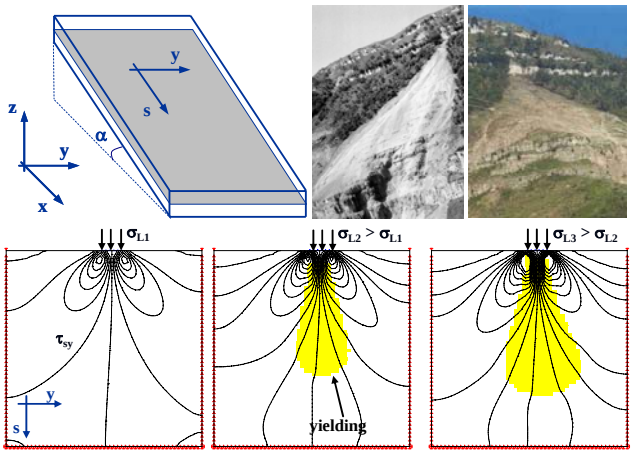

Figure 6. Stresses variations due to pressures applied at the upper boundary of a plane parallel to ground surface.

4. CONCLUSION

When involving open slopes, landslides of the flow-type often occur in triangular source areas where initial slides turn into avalanches through further failures and/or soil entrainment. Significant examples of this landslides typology were recorded in May 1998 in the pyroclastic deposits overlying the carbonate Pizzo d'Alvano massif (Southern Italy, Sarno-Quindici event). Referring to this event, the paper analyses two main triggering factors consisting in karst spring from the bedrock and impact of failed soil masses on stable deposits.

The failure stage is studied through both hydro-mechanical uncoupled and coupled approaches based on groundwater modelling, limit equilibrium and stress-strain analyses. Karst springs at the base of bedrock scarps are pointed out as a severe hydraulic boundary condition. In fact, the induced transient pore water pressures cause the failure onset mostly depending on the stratigraphy, even for short durations of the springs. Referring to the impact phenomena, the failure onset is not simulated assuming drained conditions. Conversely, in undrained conditions, the increase of pore water pressures determines the failure onset that is satisfactorily justified by limit equilibrium analyses. Analogous scenarios are obtained through stress-strain analyses that also point out the high decrease of mean effective stresses and the possibility of liquefaction phenomena.

The post-failure stage is analysed through the previous uncoupled approach based on simplified assumptions and stress-strain analyses. The achieved results outline that failure induced by karst springs from bedrock and/or impact loading can cause further failures in downslope stable deposits. Particularly, low pressures downwards acting along planes parallel to ground surface lead to yielding conditions in large portions of the hillslope whose extension and lateral enlargement depend on lateral stresses, depth and slope angle.

REFERENCES

Bilotta, E, Cascini, L., Foresta, V., Sorbino, G., Geotechnical characterization of pyroclastic soils involved in huge flowslides. *Geotechnical and Geological Engineering, 23*, 365-402, 2005.

Budetta, P., de Riso, R. The mobility of some debris flows in pyroclastic deposits of the northwestern Campanian region (Southern Italy). *Bull Eng Geol Environ, 63*, 293-302, 2004.

Calcaterra, D., de Riso, R., Evangelista, A., Nicotera, M.V., Santo, A., Scotto di Santolo, A. Slope instabilities in the pyroclastic deposits of the carbonate Appenine and the phlegrean district (Campania, Italy). *Proc. of the Int. Workshop "Flows 2003", Sorrento, Patron Ed.*, 61-75, 2004.

Cascini, L., Cuomo, S., Guida, D., Typical source areas of May 1998 flow-like mass

movements in the Campania region, Southern Italy, *Engineering Geology, 96*, 107-125, 2008.

Cascini, L., Cuomo, S., Sorbino, G., Flow-like mass movements in pyroclastic soils: remarks on the modelling of triggering mechanisms. *Italian Geotechnical Journal, 4*, 11-31, 2005.

Cascini, L., Guida, D., Nocera, N., Romanzi, G., Sorbino, G., A preliminary model for the landslides of May 1998 in Campania Region. *Proc 2nd Int. Symposium on Geotechnics of Hard Soil-Soft Rock – Napoli, Balkema, 3*, 1623-1649, 2000.

Cascini, L., Sorbino, G., Soil suction measurement over large areas: a case study. *Proc. 3rd Int. Conference on Unsaturated Soils, Recife (Brasil), Balkema 2*, 829-834, 2002.

Chen, H., Crosta, G.B., Lee, C.F., Erosional effects on runout of fast landslides, debris flows and avalanches: a numerical investigation. *Geotechnique, 56(5)*, 305-322, 2006.

Costa, J.E., Williams, G.P., Debris-flow dynamics (video tape): U.S. Geological Survey. Open-File Report 84-606., 1984.

Crosta, G., Imposimato, S., Roddeman, D.G., Continuum numerical modelling of flow-like landslides, *Landslides from Massive Rock Slope Failure, Evans et al. (eds.), Springer*, 211-232, 2006.

Cuomo, S., Geomechanical modelling of triggering mechanisms for flow-like mass movements in pyroclastic soils. *PhD dissertation at the University of Salerno, Italy*, pp. 274, 2006.

Di Crescenzo, G., Santo, A., Debris slides-rapid earth flows in the carbonate massifs of the Campania region (Southern Italy): morphological and morphometric data for evaluating triggering susceptibility. *Geomorphology, 66*, 255-276, 2005.

Fiorillo, F., Wilson, R.C., Rainfall induced debris flows in pyroclastic deposits, Campania (Southern Italy). *Engineering Geology, 75*, 263- 289, 2004.

Fredlund, D.G., Morgenstern, N.R., Widger, R.A., The shear strength of unsaturated soils. *Canadian Geotechnical Journal, 15*, 313-321, 1978.

Geoslope, User's guide. GeoStudio 2004, Version 6.13. Geo-Slope Int. Ltd. Calgary, Canada, 2004.

Gerstell, M.F., Aharonson, O., Schorghofer N., A distinct class of avalanche scars on Mars, *Icarus 168*, 122-130, 2004.

Guadagno, F.M., Forte, R., Revellino, P., Fiorillo, F., Focareta, M., Some aspects of the initiation of debris avalanches in the Campania Region: the role of morphological slope discontinuities and the development of failure. *Geomorphology, 66*, 237-254, 2005.

Guadagno, F.M., Martino, S., Scarascia Mugnozza, G., Influence of man-made cuts on the stability of pyroclastic covers (Campania-Southern Italy): a numerical modelling approach. *Environmental Geology, 43*, 371-384, 2003.

Henkel, D.J., The shear strength of saturated remoulded Clay. *Proc. of the ASCE Research Conference on Shear Strength of Cohesive Soil, Boulder, Colorado,USA*, 533-544, 1960.

Hungr, O., Evans, S.G., Bovis, M.J., Hutchinson, J.N., A review of the classification of landslides of the flow type. *Environ. and Eng. Geosci., VII (3)*, 221-238, 2001.

Hutchinson, J.N., Bhandari, R.K., Undrained loading, a fundamental mechanism of mudflow and other mass movements. *Geotechnique, 21[4]*, 353-358, 1971.

Jakob, M., Hungr, O., Debris-flow Hazard and Related Phenomena, Springer, pp. 739, 2005.

Jamiesion, B., Stethem C., Snow Avalanche Hazards and Management in Canada: Challenges and Progress, Natural Hazards 26, 35-53, 2002.

Pastor, M., Quecedo, M., Fernandez Merodo, J.A., Herreros, M.I., Gonzalez, E., Mira, P., Modelling tailing dams and mine waste dumps failures. Geotechnique, 52(8), 579-591, 2002

Pastor, M., Haddad, B., Sorbino, G., Cuomo, S., Drempetic, V., A depth integrated coupled SPH model for flow-like landslides and related phenomena. Int. Journal Numerical and Analytical Methods in Geomechanics, DOI: 10.1002/nag.705, 2008.

Pielmeier, C., Schneebeli, M., Developments in the stratigraphy of snow. *Surveys in geophysics, 24*, 389-416, 2003.

Wang, F.W., Sassa, K., Fukuoka, H., Downslope volume enlargement of a debris slide-debris flow in the 1999 Hiroshima, Japan, rainstorm. Engineering Geology, 69, 309-330, 2003.